

HIGH-TEMPERATURE RHEOLOGY OF SHS MATERIALS

L. M. Buchatskii and A. M. Stolin

UDC 621.762

Specific features of SHS materials as the objects of rheology are discussed, various types of viscosimetric flows and the choice of rheological variables are delineated, a technique of constructing isochoric rheological curves for porous bodies is illustrated, and their possible types are reported. Such factors as nonuniformity of the porosity distribution external friction, and nonisothermality of the process are considered. A compression rheometer intended for studying the compaction kinetics and rheological properties of the SHS materials is described, and data on the rheological properties of the material based on molybdenum disilicide are presented.

The development of the self-propagating high-temperature synthesis (SHS) method and its accomplishment using structural materials, superconducting ceramics, as well as tool and gradient alloys [1-8], could not but bring researchers to attempt to realize an alluring idea, viz., to produce a finished article immediately, in one stage. All the prerequisites for this were available: a refractory material that synthesizes rapidly and with heat release such that it changes to a softened state, so that by applying an external pressure the required shape and dimensions may be imparted to it.

Various authors performed studies on hot isostatic [1] and nonisostatic [2] pressing, rolling [6], and extrusion [7, 8]. Interest in such works is quite natural because, if successful, the technological process of producing the articles accelerates, costs less, and gets rid of a great number of intermediate, frequently ecologically harmful and energy-intensive stages, as compared with traditional processes in powder metallurgy.

The realization of any of the methods listed for producing the articles is based on the ability of a hot mass of the synthesized product for macroscopic flow; therefore it would be logical to refer to an SHS combination with all types of pressure treatment as rheosynthesis (from the Greek $\rho\eta\epsilon\omicron$, which means "flow"), and to divulge all secrets of producing the articles of required shape and size, and of assigned porosity relying on the knowledge of the rheological behavior of SHS products in a high-temperature region.

Rheological Characteristics of SHS Materials. The materials considered in the temperature region of our concern are specific rheological objects. They are no longer a collection of individual grains of powder but rather possess a continuous self-bound skeleton penetrated by a great number of pores of various sizes, thus resembling a sponge in outward appearance. A continual description is perfectly applicable to such objects, which also takes into account the dependence of their rheological properties on what happens to the pores and in the skeleton.

A skeleton structure may form directly in the combustion wave or far beyond it [9]. The latter causes the processes of formation of the final material structure to proceed also after the combustion has ceased, which serves as a prerequisite for the variation, during deformation, of such structure-sensitive properties of the material as viscosity or yield point. Depending on the duration and depth of the processes of structural transformations, not only the nonlinearity degree of the rheological behavior may alter but a combination of various rheological properties such as viscosity, plasticity, and elasticity will manifest itself as well after the synthesis wave has passed.

Let us run down the influence of porosity, taking, as a case in point, the viscous behavior of the compressible medium considered in detail when describing the processes of hot pressing and sintering of powder materials [10]. A simultaneous change in the shape and size of the body is determined by its two characteristics, viz., by dilatational and shear viscosities. In shear flows with only tangential stresses acting, only the shear viscosity reveals itself. As for compressible materials, it is important to first

study their capability for compaction. A significant role is played here by the dilatational viscosity and its dependence on the porosity. In the continual model of a compressible liquid, the following relations for the shear η and dilatational ζ viscosities are introduced:

$$\eta = \eta_s \varphi(\Pi), \quad \zeta = \eta_s \psi(\Pi), \quad (1)$$

where η_s is the viscosity of the material of a skeleton without pores, Π is the volume fraction of pores throughout the volume of a porous body, and φ and ψ are the porosity functions established experimentally. With vanishing porosity, the shear viscosity of the porous body tends to that of the skeleton material η_s , whereas the dilatational viscosity increases to infinity, which is in compliance with the condition of incompressibility of the skeleton material. Such behavior is most often defined by the porosity functions in a power-law form:

$$\varphi(\Pi) = (1 - \Pi)^m; \quad \psi(\Pi) = 2(1 - \Pi)^\alpha / 3\Pi, \quad (2)$$

in which the parameters m and α generally assume values lying within several units. We should point out that similar considerations are used to determine the elasticity modulus of the compression strength or various effective transfer coefficients in heterogeneous media [11].

The above-mentioned specific features of the SHS materials in comparison with the objects of classical rheology, in view of the nonstationarity of their compression, make it impossible in principle to apply the familiar schemes and techniques of experimental rheology, and compel one to choose anew viscosimetric flows, rheological coordinates, devices, and methods for solving the inverse problem. It is the solution of the above-stated problems along with the development of the instrumental base and the accumulation of experimental data, including those on the dynamics of structural transformations during deformation, that make up the contents of a novel scientific trend, namely, that of high-temperature rheology of SHS materials.

The present study gives a review of the studies which may be related to the initial steps of solving each of the above-stated problems.

Viscosimetric Flows and Rheological Variables. Among the possible methods of pressure treatment of porous materials, those that may be referred to as viscosimetric, which allow one to obtain information on dilatational and shear viscosities, are described by relatively simple and readily solved equations, and admit a simple experimental realization: 1) linear axial compression in a cylindrical mold, 2) radial compression between long coaxial cylinders, and 3) uniform compression.

During the isothermal process and in the case with no friction against the pressing tool, the flow types listed are characterized by the presence of only one nonzero component of the velocity vector v_z and of one nonzero component of the deformation rate tensor $\partial v_z / \partial z$. Here, invariants of the deformation rate tensor are dependent only on this component: $J_s = (\partial v_z / \partial z)^2$, and any dependence of the viscosities on the deformation rate reduces to that on the velocity gradient, readily determinable experimentally for a uniform deformation.

As an illustration of various questions involved in analyzing the rheological behavior of SHS materials, let us consider the simplest case of the isothermal uniform compression of a viscous porous medium in a rigid cylindrical mold, without friction on the side walls. The compression is defined by the following system of equations:

of continuity

$$\frac{d(1 - \Pi)}{dt} = -\frac{1}{1 - \Pi} \frac{\partial v_z}{dz} = -\frac{e}{1 - \Pi}, \quad (3)$$

and of balance:

$$\partial \sigma_s / \partial z = 0, \quad (4)$$

whereas the equation of state for the main components of the stress tensor is brought into the form

$$\sigma_z = \eta_s (4\varphi/3 + \psi) e; \quad (5)$$

$$\sigma_r = \sigma_\theta = \eta_s (-2\varphi/3 + \psi) e. \quad (6)$$

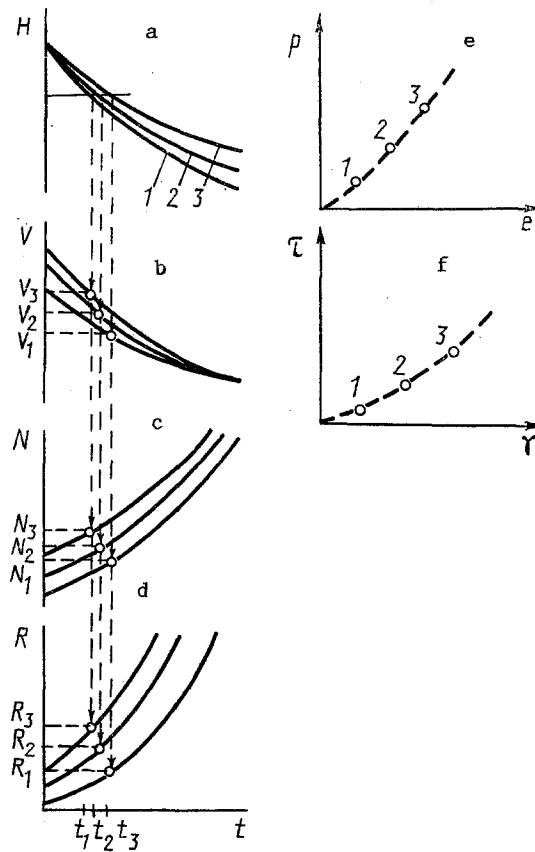


Fig. 1. Procedure of constructing the rheological curves from the data of a run of three viscosimetric experiments (numerals by the curves (a) and by the points (e,f) denote numbers of the experiments).

Since the deformation is uniform, in accordance with [12], all variables inside the volume are uniform and equal to their proper boundary values. Let us use this fact in writing the solution to the system (5)-(6):

$$N = \eta_s (4\varphi/3 + \psi) (V/H), \quad (7)$$

$$R = \eta_s (-2\varphi/3 + \psi) (V/H). \quad (8)$$

The relations (7) and (8) point to a set of four viscosimetric variables to be determined from the experiment, viz., the pressure on the die N , the lateral pressure R , and the specimen height H related directly to its relative density $\rho = 1 - \Pi$, $\rho H = \rho_0 H_0$, and to the rate of variation in this height V . With allowance made for $V = dH/dt$, the measured values of $N(t)$, $R(t)$, and $H(t)$ are sufficient for investigating the rheological properties.

Studying the kinetics of material compaction $H(t)$ as well as other relations, for example, $N(H)$, $N(V)$, $R(H)$, and $V(H)$ is of practical interest because these are compaction characteristics of one or another material and of its pressing mode. However, they must be treated taking into account the variation in the characteristics at hand, viz., in the process time, porosity, velocity, etc. Besides, the indicated characteristics intricately incorporate a combination of the shear and dilatational viscosities of the material.

From the above set of viscosimetric variables we ought to find the so-called rheological variables, the relation between which might be utilized for predicting the properties and would be sensitive to the porosity variation. Such variables for incompressible materials are the shear stress and rate, and the relation between them (a flow curve) determines the shear viscosity and its dependence on deformation parameters [13].

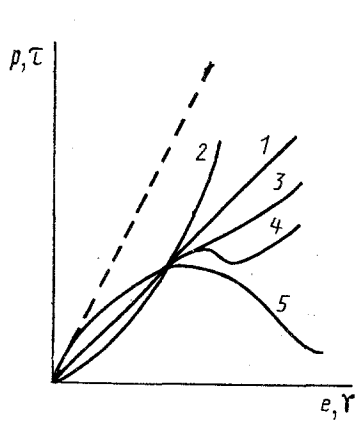


Fig. 2

Fig. 2. Possible types of rheological curves of a viscous porous material at various porosities (dashed line) and indexes of non-Newtonian behavior (solid lines).

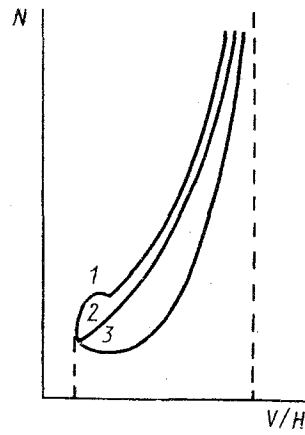


Fig. 3

Fig. 3. Viscosimetric characteristics of linear compression for pseudoplastic (curves 1 and 3) and dilatational (curve 2) materials.

The rheological variables for compressible media must, of course, be sought among the invariants of stresses, deformations, and deformation rates. This question was covered most consistently and comprehensively in [14], whence we borrow the following relationships to define the dilatational and shear viscosities:

$$p = \eta_{ef} \psi e; \quad \tau = \eta_{ef} \varphi \gamma, \quad (9)$$

where p , τ , e , and γ are the first and the second invariants of the stress tensors and of the deformation rates, respectively:

$$p = \sigma_{ij} \delta_{ij} / 3; \quad \tau = \sqrt{(\sigma_{ij} - p \delta_{ij})(\sigma_{ij} - p \delta_{ij})}, \\ e = e_{ij} \delta_{ij}; \quad \gamma = \sqrt{(e_{ij} - e \delta_{ij} / 3)(e_{ij} - e \delta_{ij} / 3)}$$

(η_{ef} is the effective viscosity of the skeleton material to be defined).

In the case of pressing considered, $e = -V/H$, $\gamma = (2/3)^{1/2} V/H$, $p = -(N + 2R)/3$, and $\tau = -(2/3)^{1/2}(R - N)$, and expressions (7) and (8) take on the following form:

$$N + 2R = 3\eta_{ef} \psi V/H, \quad (10)$$

$$N - R = \eta_{ef} \varphi V/H. \quad (11)$$

Constructing the rheological curves $p - e$ and $\tau - \gamma$ allows us to determine the dilatational and shear viscosities for the porous medium, but here we fail to get rid of the porosity, varying along the above-mentioned curves.

Construction of Rheological Curves. A procedure for constructing the rheological curve for a specified porosity was first delineated in [15]. Its construction requires a run of j experiments, in each of which the initial value of any of the parameters varies, viz., of the pressure N , the velocity V , and the initial height H_0 . Figure 1 shows the construction of the rheological curve from the data of viscosimetric experiments for $j = 3$.

From the curves of compaction kinetics $H_j(t)$, a certain specimen height H is selected, corresponding in this case to a definite relative density ρ or porosity Π (Fig. 1a), and at appropriate time instants t_j (the time of attaining the assigned H in each experiment), the quantities V_j , N_j , and R_j , which are needed for calculating the rheological parameters p_j , τ_j , e_j , and γ_j , are identified. Thus, we obtain the isochoric rheological curves $p_j - e_j$ and $\tau_j - \gamma_j$, along which the density and the porosity do not alter.

By iterating this procedure for another height of the specimen blank, we may get a set of rheological curves with porosities different but unchanging along each of them. A porosity decrease results in an increase in the angle of inclination to the axis e or γ .

In the compaction method investigated, only one of the stress tensor components, e.g., the axial pressure, can act as one of the rheological variables. The rheological curve $N_j - e_j$ or $N_j - \gamma_j$, similarly to those considered previously, may be obtained from the experimental run conducted by the procedure described. A qualitative form of the curves $N - e, \gamma$ does not differ from $p - e$ and $\tau - \gamma$; however, the ratio of the pressure to any component of the deformation rate tensor defines, up to a constant factor, a certain effective quantity, i.e., a measure of resistance in linear compression. In conformity with Eq. (7), it combines both viscosities additively. Nevertheless, appropriate parameters of the power-law relation form and α may be selected for their porosity functions, and the inverse problem of defining these functions and η_e may be solved. In principle, the lateral pressure R is also suitable for these purposes, but its experimental measurement is more complicated.

It is not difficult to demonstrate that the parameters m and α have a slight (even quantitative) effect on the rheological curves. For a qualitative analysis of the influence of porosity on the flow properties and regularities for such materials, we can restrict ourselves to simple forms of the porosity functions φ and ψ , e.g., to set $m = 1$ and $\alpha = 0$ or 1 . The inverse proportionality of the dilatational viscosity and the material porosity is crucial. As a porous state is approached, all specific features of the stress-strain state and of the compaction kinetics are connected precisely with this relation.

All the aforesaid pertains to the linear-viscous compressible body, and only a straight line in isochoric coordinates might be obtained as the rheological curve (Fig. 2, curve 1). Analyzing the possible types of rheological curves for a non-Newtonian behavior of the material is a direct problem of rheology. Below, we will examine a nonlinear-viscous behavior which is due to the dependence of the effective viscosity on the deformation rate.

As has already been noted, the viscosimetric flows are characterized by the presence of only one component of the deformation rate tensor, just to the dependence on which the rheological equation of state must be reduced. Here, a power-law form of this dependence is most commonly used:

$$\eta_{ef} = \eta_s W^{n-1}, \quad W = \sqrt{\psi e^2 + \varphi \gamma^2} / \sqrt{1 - \Pi}, \quad (12)$$

where W is the equivalent deformation rate [14]. For a specified porosity Π_* , it may be represented as $W_* = e_f(\Pi_*) = \gamma_f(\Pi_*)$, where $f_e(\Pi_*)$ and $f_\gamma(\Pi_*)$ are readily computed parameters. On substituting all this, together with Eq. (12), into (9) we acquire the following expression for the rheological curves:

$$p = \zeta_{ef} e^n, \quad \tau = \eta_{ef} \gamma^n, \quad (13)$$

$$\zeta_{ef} = \eta_s \psi(\Pi_*) f_e(\Pi_*); \quad \eta_{ef} = \eta_s \varphi(\Pi_*) f_\gamma(\Pi_*).$$

The case $n = 1$ conforms to the above-considered linear behavior. The value $n > 1$ implies a viscosity increase with advancing deformation. Following [16], we will refer to media of such kind as dilatational. Experimental data [10] indicate that among these are the majority of powders of refractory compounds and alloys. The dilatational materials are characterized by the rheological curves $p - e(\tau - \gamma)$ monotonically increasing throughout the range of possible porosities (Fig. 2, curve 2).

A viscosity reduction with increasing deformation ($n < 1$) conforms to a pseudoplastic behavior [16]. Most polymers and, therefore, powder compositions based on them exhibit such distinctive features of the rheological behavior. Their rheological curves are distinguished by a great diversity, i.e., nonmonotonic ones are also encountered among them (Fig. 2, curves 3-5). This diversity is due to competitiveness between the material stress rise in the material and the viscosity fall as the velocity gradient increases. If the relation $\eta_e(W)$ is weak and rapidly saturated, a point of inflection appears on the monotonically growing curve (Fig. 2, curve 3). In case the viscosities at small and large velocity gradients differ significantly, two extrema arise on the rheological curve (Fig. 2, curve 4). If the viscosity reduction does not cease in the range of W considered, the rheological curves pass through a maximum (Fig. 2, curve 5). The noted regularities do not change on going from one porosity value to another. Accurate quantitative calculations for the extrema coordinates, points of inflection, and for other characteristics of the rheological curves are feasible provided the form and parameters of the relation $\eta_e(W)$ are known.

It should be noticed that distinctions between the dilatational and pseudoplastic behavior of the material may be discovered even from a single experiment. For this, it must be performed at a constant pressing rate, and the characteristic $N(e)$ must be analyzed (Fig. 3). Nonmonotonic curves 1 and 3 of the porosity (dashed line) and of the index of non-Newtonian behavior (solid lines) are characteristic only of the pseudoplastic materials and caused by the competitive influence exerted on the viscosity by two factors, i.e., by the viscosity decrease owing to increasing deformation rate and by the viscosity increase due to the porosity reduction. The latter always leads to an increase in $N(e)$ at the end of the process, but the initial stages of the compaction due to the first factor can proceed with a reduction of the stress acting in the material.

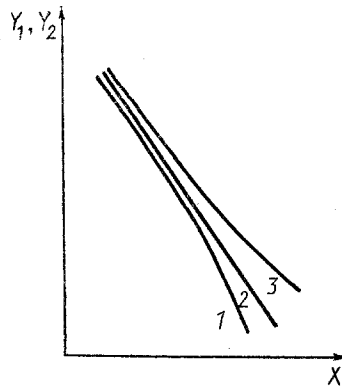


Fig. 4. Representation of the experimental curves in rectification coordinates.

During the compaction of the dilatational materials, both factors noted entail a rise in the effective viscosity; therefore, the curves $N(e)$ in the regime of deformation with a constant-rate pressing are always monotonic (Fig. 3, curve 2).

Defining the material properties from the experimental data makes up the subject of the inverse problem of rheology. Based on the solution of the direct problem, the following technique may be suggested for predicting the rheological properties. In the general case, it involves several stages. The relations, measured in the experimental run, are taken to be the original experimental material. Within the porosity range, a collection of the values of Π_j is selected, for each of which the isochoric rheological curves $p_j - e_j$ and $\tau_j - \gamma_j$ are constructed according to the above-described procedure. They permit one to determine, in double logarithmic coordinates, an effective value of the viscosity appropriate for the chosen porosity:

$$\begin{aligned} \ln p_j &= \ln \zeta_{\text{ef}j} + n \ln e_j, \\ \ln \tau_j &= \ln \eta_{\text{ef}j} + n \ln \gamma_j. \end{aligned} \quad (14)$$

Repeating this procedure for each selected porosity value and adopting a power-law form of the porosity functions (2), we obtain the parameters of these relations:

$$\ln \eta_{\text{ef}} = \ln \eta_s + m \ln (1 - \Pi). \quad (15)$$

If the assumption on a "power" law of the flow is fulfilled, all parameters may be determined from one experiment. Combining the equations yields the following equations:

$$N + 2R = \eta_s 2 \frac{(1 - \Pi)^{m+1}}{\Pi} \sqrt{\frac{2}{3} \frac{(1 - \Pi)^{m-1}}{\Pi}} \left(\frac{V}{H}\right)^k, \quad (16)$$

$$N - R = \eta_s (1 - \Pi)^m \sqrt{\frac{2}{3} \frac{(1 - \Pi)^{m-1}}{\Pi}} \left(\frac{V}{H}\right)^k, \quad (17)$$

each of them containing only three unknown parameters. The latter may be defined in the corresponding coordinates:

$$Y_1 = \ln \left[\frac{(N + 2R) \sqrt{\Pi^3}}{2 \sqrt{\frac{2}{3} (V/H)^k}} \right], \quad X_1 = \ln (1 - \Pi), \quad (18)$$

$$Y_2 = \ln \left[\frac{(N - R) \sqrt{\Pi}}{\sqrt{\frac{2}{3} (V/H)^k}} \right], \quad X_2 = \ln (1 - \Pi). \quad (19)$$

By varying the nonlinearity exponent k , as yet unknown, the experimental data can be represented as a straight line, whose inclination angle defines the parameters $(3m + 1)/2$ or $(3m - 1)/2$, and intercept determines the quantity η_s . A notable feature of the proposed technique is a rectification of the experimental curve only provided the nonlinearity exponent is chosen correctly, i.e., $k = n$ (Fig. 4, curve 2). If the selected k is smaller than the true value ($k < n$), the experimental curve in the indicated coordinates, in the region of low porosity, will deflect downwards (Fig. 4, curve 1), whereas with the chosen k larger than the true value ($k > n$), it will deflect upwards (Fig. 4, curve 3).

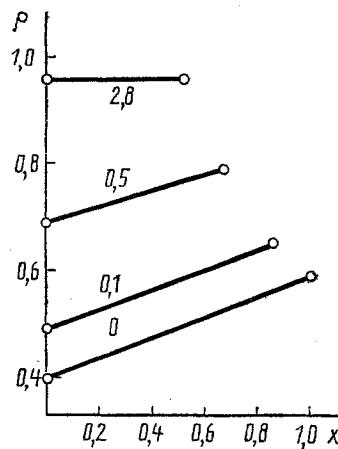


Fig. 5. Distribution of relative porosity in the specimen during nonuniform compression. Numerals by the curves denote dimensionless time.

The technique suggested presumes measurements of the axial and lateral pressure, of the specimen height, and of its variation rate in each experiment on linear compression of the porous material. However, the material properties may be identified by measuring only two quantities, viz., $N(t)$ and $H(t)$. The velocity is found through differentiating the latter curve. The curves $N - e$, constructed afterwards for various porosities in the coordinates $N - \ln e$, will determine the degree of non-Newtonian behavior and the porosity dependence of the effective resistance to the linear compression, which combines in an additive manner the shear and dilatational viscosities of the porous body.

If the material manifests non-Newtonian properties, it does not appear possible to divide the obtained resistance measure into dilatational and shear components. However, in view of the weak effect of the parameters m and α on the rheological curve, both viscosities may be evaluated with good accuracy, assuming $m = \alpha$.

In case the material behavior is Newtonian, the problem of determining the parameters may be solved completely using an exact solution for the initial equations [15].

Both of the outlined methods (based on a complete and a reduced set of measured parameters) have merits and demerits. Measuring the complete set of parameters is a task more difficult to accomplish experimentally but the results obtained thereby are independent of the initial theoretical notions. Alternatively, rather general assumptions on the power-law form of sought relations, which enabled obtaining of the rectification coordinates, and simplicity of the experimental implementation are the merits of the second method. The method presented of ascertaining the index non-Newtonian behavior is applicable to arbitrary, including noninteger, values of n , which gives it an advantage over the method given in [10].

Influence of Various Factors. The above-described analysis of the rheological behavior was carried out under the assumption of the deformation uniformity (directly relating to the uniformity of porosity distribution over the specimen), the absence of external friction on contacts with the pressing equipment, and of the process isothermality. In reality, these assumptions may not be satisfied; therefore, all the above-mentioned factors must be analyzed, which is of undoubted methodical interest.

Porosity Nonuniformity. The solution of a relevant problem [17] revealed that a distortion of results due to the porosity nonuniformity is the greatest only at the initial instant of time. A nonuniform initial distribution of the porosity causes a nonuniform stress-strain state of the material, which tends to equalize the porosity at different points of the volume. Figure 5 shows the transformation of the initial linear porosity distribution during the compaction.

A porosity self-equalization over the material volume is due to the compaction deceleration with decreasing absolute value of the porosity. As a consequence, the microvolumes with increased porosity diminish it rapidly, and the pore distribution vanishes. Predictions show that, after a short time, the nonequidensity discontinues affecting the viscosimetric curves.

External Friction. In [18] we studied various facets of the effect of external friction on the compaction regularities for porous materials in hot pressing; here we will dwell only on methodical aspects of measuring the properties of SHS materials.

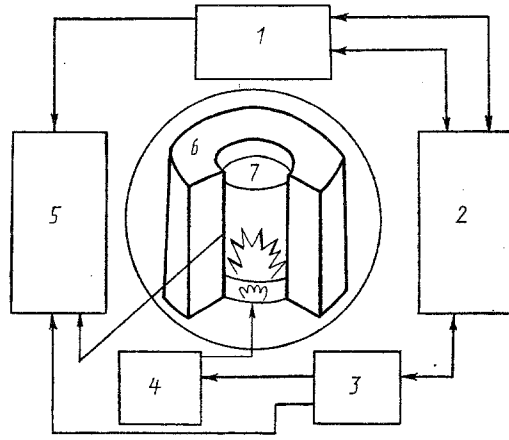


Fig. 6. Schematic of the compression rheometer: 1) loading device; 2) pneumatic distributor; 3) mode controller; 4) ignition unit; 5) recording unit; 6) measuring unit; 7) tested specimen.

The material friction against a working tool at high temperatures is a complex and multifactor phenomenon by itself. For estimating its influence on the process of measuring the properties, it is sufficient to restrict ourselves to a region of moderate and weak friction. Of primary importance in this region is the dependence of the friction force on a multiply increasing, during the compaction, normal component of the stress tensor to the friction surface, and the direction of the friction force, governed by the relative velocity of the material movement over the pressing equipment. Taking account of these factors has necessitated consideration of the second, i.e., radial component of the velocity vector, and of the corresponding second balance equation and additional boundary conditions:

$$r = 0: V_r = 0; \partial v_r / \partial r = \partial v_z / \partial r = 0;$$

$$r = R: \tau_{rz} = f \operatorname{sign}(v_z - v_c) \sigma_{rr}.$$

However, assuming the friction coefficient f is small, we managed to reduce the problem, with the aid of averaging, to a one-dimensional formulation relative to radius-average variables. The analysis of this problem displayed that uniformity of all characteristics over the volume is not actually disturbed in the complex parameter region $fH_0/2R < 0.5$. Hence, to conduct the measurements one should use specimens with a height-to-diameter ratio not larger than unity.

Nonisothermal Conditions. The organization of measurements of the rheological properties for SHS materials implies by itself their combustion-mode synthesis, which makes it necessary to allow for or use the process nonisothermality. Under the conditions when synthesis has terminated, nonisothermality may be caused by the specimen cooling, by exo- or endothermicity of the processes of final structure formation, and by the dissipative heat release. A heat mode of the porous mass deformation will be specified in these conditions by the relationships between the characteristic times of cooling $t_0 = c\rho_s H_0/\alpha_T$, compaction $t_c = 4\eta_s/3N$, dissipative heat release $t_d = 4\eta_s c\rho_s/N^2$, and of the thermal effect of structural transformations t_{str} . The maximal possible dissipative heating in the system can amount to a value of the order of $N/c\rho_s$, which introduces an error within the measurement accuracy in the temperature interval considered [19], and therefore may be ignored. Estimates of the thermal effects for the process of structural transformations also allow one to disregard this factor. A maximal distortion of the results may result from the modes of strong cooling after the combustion wave has passed. But here there is also a fairly vast region of the parameters δ , viz., $\delta < 10^{-3}$ [20], where a quasi-isothermal compaction mode can be realized, with which very insignificant temperature variations occur in the material and which can be used to perform the viscosimetric measurements, referring the results to a temperature average over the experiment time.

A disturbance of this mode leads to a self-accelerated cooling of the material, caused by the positive feedback between the temperature fall, the increase in resistance to the compression, and the compression deceleration, and to a still greater temperature fall over this time.

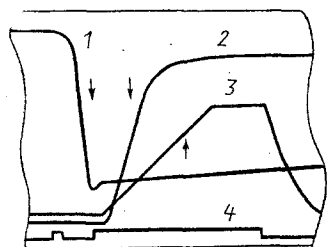


Fig. 7

Fig. 7. Typical oscillogram of the process: 1) temperature; 2) movement of the pressing plunger; 3) pressure; 4) time intervals. Arrows by the curves indicate the direction of growth of the variables.

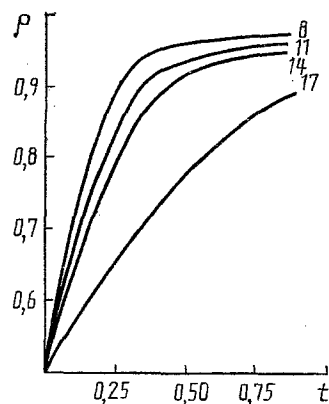


Fig. 8

Fig. 8. Compaction kinetics of a material based on molybdenum disicilide measured at various delay times after the initiation until the moment of pressure application (see numerals by the curves).

Rheometry of SHS Materials. For laboratory investigations of compaction processes of SHS materials and for measuring their rheological properties in the combustion temperature range, a compression rheometer is created, which ensures initiation and execution of the SHS process, loading of the combustion products at a specified instant of time or, after a designated temperature is attained, a recording in time of dynamic and kinematic characteristics for the compression process of a hot porous mass [21]. In order to provide reproducibility of the combustion process, allowance is made for automatically conducting the experiment under the prearranged program. The device can also be employed for studying the compaction kinetics of inert porous powder materials.

The rheometer has the following specifications: a generated force of 0.2-12 tons (2-120 kN), a pressing rate of 1-100 mm/sec, a pressure in the loading device chamber of 10-150 atm, a measuring unit pressure of 0.1-5 kbar, and a working temperature of 1000-3000 K.

A schematic of the rheometer is shown in Fig. 6. It consists of a device for loading with a prescribed pressure, a pneumatic distributor, a measuring unit, an ignition unit and a mode controller, and a recording unit, which utilize some unconventional engineering solutions [22, 23].

The loading device represents a pneumatic cylinder, by means of which the force is generated. The pneumatic distributor allows one to maintain a constant gas pressure of up to 150 atm in the chamber of the pneumatic cylinder, and redistribution of the gas flows for pressing and for lifting a plunger.

The measuring unit is a power chamber with electric leads of the initiation device, antifriction ring, and of the die. A pellet of the material studied is located inside the ring.

The ignition unit permits initiation of the combustion reaction on one or both sides by a tungsten spiral or a high-voltage discharge. The latter appreciably reduces the combustion time and the residual temperature gradient, and improves the measurement correctness.

The mode controller allows one to select one of four pressing modes: 1) at an assigned delay time after the initiation moment; 2) on heating to a designated temperature; 3) on cooling to a designated temperature; and 4) for the inert material.

The experiment is executed as follows. A prepressed pellet of the original charge of the material considered, 30 mm in diameter and height, is placed into the power chamber of the measuring unit, the combustion is initiated therein, and after it has terminated the workpiece is compacted under the action of an assigned force under the conditions of linear compression. During the experiment, we registered the temperature, the pressure, and the plunger movement, which is readily converted to the relative density and porosity. Figure 7 gives a typical oscillogram of the process.

As an illustration of the method outlined, Fig. 8 presents the compaction kinetics for one of the compositions based on molybdenum disilicide, measured by I. V. Usovich at various delay times after the initiation till the moment of pressure application. As this time lengthens, the material temperature falls due to cooling; therefore, with increasing t_d the compaction decelerates, while the residual porosity grows.

The derived data on compaction kinetics were processed with the aid of the procedure put forward above. The processing results showed that all the data satisfy the power-law form of the rheological equation of state

$$p = \eta_0 \exp\left(\frac{U}{RT}\right) W^{n-1} \dot{\epsilon}; \quad \tau = \eta_0 \exp\left(\frac{U}{RT}\right) W^{n-1} \dot{\gamma}$$

with the following parameters: $\eta_0 = 92 \text{ (Pa} \cdot \text{sec)}^{1/n}$, $U/R = 1.6 \cdot 10^4 \text{ K}$, and $n = 0.2$. In the temperature range of 1800-1300°C, the shear viscosity of the incompressible base varies from 10^6 up to $8 \cdot 10^6 \text{ Pa} \cdot \text{sec}$.

LITERATURE CITED

1. O. Odawara and Y. Kaieda, *Sosei to Kako*, **28**, No. 312, 3-8 (1987); O. Odawara and Y. Kaieda, *Trans. Nat. Res. Inst. Metals*, **30**, No. 2, 18-24 (1986); G.Y. Richardson et al., *Ceram. Eng. Sci.*, **7**, Nos. 7-8, 761-770 (1986).
2. A. G. Merzhanov, I. P. Borovinskaya, et al., in: *Scientific Fundamentals of Study of Materials [in Russian]*, Moscow (1981), pp. 193-206.
3. A. G. Merzhanov, I. P. Borovinskaya, M. D. Nersesyan, et al., *Dokl. Akad. Nauk SSSR*, **311**, No. 1, 96-101 (1990).
4. N. Sata, *J. Ind. Expl. Soc. Jpn.*, **49**, No. 4, 242-249 (1988).
5. A. N. Pitulin, Yu. M. Bogatov, and A. S. Rogachev, *Abstracts of the 1st International Symposium on SHS, Alma-Ata, 1991*, p. 154.
6. R. W. Rice et al., *Ceram. Eng. Sci.*, **7**, Nos. 7-8, 751-756 (1986).
7. A. G. Merzhanov, A. M. Stolin, V. V. Podlesov, et al., *A Method for Fabricating Articles from Powder Materials and a Device for its Implementation [in Russian]*, USA Patent No. 5 053 192.
8. A. G. Merzhanov, A. M. Stolin, L. M. Buchatskii, et al., *A Ceramic Composite Material and a Method of Its Production [in Russian]* European Patent No. 89910469.9 of April 15, 1991.
9. A. G. Merzhanov, *Pure Appl. Chem.*, **62**, No. 5, 861-875 (1990).
10. M. S. Koval'chenko, *Theoretical Basics of Hot Pressing of Porous Materials [in Russian]*, Kiev (1986).
11. *Physical Study of Materials in the USSR [in Russian]*, Kiev (1986).
12. L. M. Buchatskii, A. M. Stolin, and S. I. Khudyaev, *Poroshk. Metall.*, No. 9, 37-42 (1986).
13. G. V. Vinogradov and A. Ya. Malkin, *Rheology of Polymers [in Russian]*, Moscow (1977).
14. V. V. Skorokhod, M. B. Shtern, I. F. Martynova, *Poroshk. Metall.*, No. 8, 23-30 (1987).
15. L. M. Buchatskii and A. M. Stolin, *Inzh.-Fiz. Zh.*, **57**, No. 4, 645-652 (1989).
16. Z. Tadmor and K. Gogos, *Theoretical Basics of Polymer Processing [in Russian]*, Moscow (1984).
17. L. M. Buchatskii, A. M. Stolin, and S. I. Khudyaev, *Poroshk. Metall.*, No. 12, 9-14 (1987).
18. L. M. Buchatskii, S. V. Khudyaev, and G. V. Shkadinskaya, *Hot Pressing of Powder Material with a Nonuniform Density Distribution under the Conditions of Dry Friction. Preprint Branch of the Institute for Chemical Physics, USSR Academy of Sciences, Chernogolovka* (1988).
19. L. M. Buchatskii and A. M. Stolin, *Abstracts of Reports, Second All-Union Conf. "Rheology and Optimization of Polymer Processing," Part 2, 107-111 [in Russian]*, Izhevsk (1989).
20. L. M. Buchatskii and A. M. Stolin, *Poroshk. Metall.*, No. 5, 24-28 (1992).
21. L. M. Buchatskii, Sh. N. Nadrshin, and A. M. Nagnii, in: *Silicides and Their Application in a High-Temperature Range [in Russian]*, Kiev (1990), pp. 55-58.
22. V. V. Podlesov, L. M. Buchatskii, V. P. Kashanskii, et al., "A hot-pressing device," *Inventor's Certificate No. 1223515 of May 10, 1984*.
23. L. M. Buchatskii and Sh. N. Nadrshin, *A Method for Igniting an Exothermal Charge. Positive Decision on Application No. 4804019/02 of March 21, 1990*.